Available online at www.sciencedirect.com
ScienceDirect
Biomaterials 29 (2008) 185–192
Biomaterials
www.elsevier.com/locate/biomaterials

Novel scaffolds fabricated from protein-loaded microspheres for tissue engineering

Ana Jaklenec, Eugene Wan, Maria E. Murray, Edith Mathiowitz*

Center for Biomedical Engineering, Brown University, Providence, RI 02912, USA

Received 19 June 2007; accepted 18 September 2007

Abstract

Biodegradable scaffolds play an important role in tissue engineering by providing physical and biochemical support for both differentiated and progenitor cells. Here, we describe a novel method for incorporating proteins in 3D biodegradable scaffolds by utilizing protein-loaded microspheres as the building blocks for scaffold formation. Poly(L,D-lactic-*co*-glycolic acid) (PLGA) microspheres containing bovine serum albumin (BSA) were fused into scaffolds using dichloromethane vapor for various time intervals. Microspheres containing 0, 0.4, 1.5, 4.3% BSA showed that increased protein loading required increased fusion time for scaffold fabrication. Protein release from the scaffolds was quantified *in vitro* over 20 days and compared to that of loose microspheres. Scaffolds had a slightly lower (up to 20%) release over the first 10 days, however, the cumulative release from both microspheres and scaffolds at the end of the study was not statistically different and the rate of release was the same, indicating that microsphere release can be predictive of scaffold kinetics. Scaffolds fused from larger ($113.3 \pm 58.0\,\mu m$) rather than smaller ($11.15 \pm 11.08\,\mu m$) microspheres, generated pores on the order of 200 μm as compared to 20 μm, respectively, showing control over pore size. In addition, four dyes (carbon black, acid green, red 27, and fast green FCF) were encapsulated in PLGA microspheres and fused into homogeneous and partitioned scaffolds, indicating control over spatial distribution within the scaffold. Finally, the scaffolds were seeded with fibroblast cells, which attached and were well spread over the polymer surface after 4 h of incubation. These results highlight the versatility of this simple scaffold fusion method for incorporating essentially any combination of loaded microspheres into a 3D structure, making this a powerful tool for tissue engineering and drug delivery applications.

Keywords: Biodegradable; Cell adhesion; Controlled drug delivery; Microsphere; Protein; Scaffold

1. Introduction

Tissue engineering has emerged over the last several decades as a possible therapy for damaged tissues and organs [1]. A common approach utilized by several laboratories [2–7] has focused on seeding cells onto 3D porous scaffolds in order to guide tissue regeneration. These constructs are then either cultured *in vitro* until functional enough for implantation or they are implanted right after cell seeding and allowed to develop *in situ*. The scaffold can serve as a temporary artificial matrix until the cells synthesize their own, or it can become integrated with the cells and provide structural support long term. There are several criteria for an ideal scaffold based on practical issues regarding handling and implantation as well as from empirical data [6]. The main requirement is high porosity (including adequate pore size) in order to allow for cell seeding, cell migration, diffusion and transport of nutrients and waste products in and out of the scaffold. Second, the scaffold needs to promote cell attachment and be biocompatible in order to prevent inflammation, scarring and induce proper integration with host tissue. Control of scaffold biodegradability is also very important as its degradation needs to be coupled with cell proliferation and matrix synthesis. Furthermore, the entire cell/scaffold construct must be appropriate for surgical manipulation. Finally, the ability to program the scaffold prior to

*Corresponding author. Tel.: +1 401 863 1358; fax: +1 401 863 1595.
E-mail address: Edith_Mathiowitz@brown.edu (E. Mathiowitz).

0142-9612/$ - see front matter © 2007 Published by Elsevier Ltd.
doi:10.1016/j.biomaterials.2007.09.017

implantation with biochemical signals can be advantageous if one is trying to recruit cells, and has become an important requirement for stem cells or progenitor cells differentiation *in situ* [3].

Growth factor signaling is very important in embryonic and developmental cell biology as well as in tissue repair processes [8]. For example, stem cell differentiation on 3D PLGA scaffolds is greatly enhanced by growth factor dosing [3]. Therefore, scaffolds that can direct cellular function via biochemical signals are likely to be useful to tissue engineering. Several groups have developed methods to deliver growth factors in scaffolds and shown that they can be released in bioactive form [7,9–20]. However, in many cases, the growth factors are simply mixed with or absorbed on to the biomaterial and the release kinetics are not precisely known or controlled [7,21–33]. Mooney et al. [2] have developed alginate hydrogels that can release growth factors when triggered by mechanical stimulation, emphasizing the importance of responsive systems. They have also fabricated dual growth factor releasing scaffolds and shown their angiogenic potential [15]. These studies demonstrate the importance and need for controlled release of a wide range of drugs and proteins from a single construct or scaffold.

Therapeutic sustained growth factor delivery has been available clinically for more than a decade. For example, human growth hormone encapsulated in PLGA microspheres is available for local injectable delivery from ProLease® (Alkermes, Cambridge, MA). Due to incredible interest by the pharmaceutical industry to develop such delivery systems a great research effort has been devoted to formulations that stabilize and deliver growth factors over long term. PLGA microspheres have been by far the most popular delivery vehicle for several reasons. PLGA is a copolymer of lactic and glycolic acid monomers and adjustment of their ratio allows tailoring of the polymer degradation rate from a few weeks to up to a year [34]. Furthermore, PLGA has a history of clinical use in resorbable sutures, bone plates and extended release pharmaceuticals. Therefore, it seems advantageous to develop a protein delivery scaffold based on microsphere encapsulation technologies.

Our goal is to develop a simple and unique method for fabricating 3D scaffolds from protein loaded microspheres. While others have incorporated microspheres into their scaffolds or hydrogels [7], here we describe a scaffold fusion method where the microsphere itself is the building block. The work presented describes how various parameters, such as fusion time, microsphere composition and size, affect the resulting scaffold structure and morphology. In addition, we highlight how scaffold composition can be tailored from essentially any loaded microspheres and how microsphere (i.e. drug) distribution can be controlled within the scaffold. Furthermore, we show that this scaffold can also act as a cell carrier, emphasizing its potential in tissue engineering applications.

2. Materials and methods

2.1. Materials

Poly(L,D-lactic-*co*-glycolic acid) (PLGA, RG502 H) was purchased from Boehringer Inglheim, Germany and used as supplied. Poly(vinyl alcohol) (PVA, 88% hydrolized, mw~25,000) was purchased from Polysciences Inc, Warrington, PA. Bovine serum albumin (BSA) (98%), fast green FCF and acid green 25 were obtained from Sigma-Aldrich, St. Louis, MO. Raven carbon 1200 and red 27 were purchased from Columbian Chemicals Company, Marietta, GA and Rachel's Supply, Gautier, MS, respectively. Dichloromethane (CH_2Cl_2) and 2,2,2-trifluoroethanol (TFE) were reagent grade.

2.2. Microsphere fabrication

Microspheres containing BSA or dyes were fabricated using a spontaneous emulsion (SE) method [35]. Relatively small and large size distributions were fabricated. For the smaller sized microspheres, 200 mg of PLGA were dissolved in 5 mL of co-solvent (CH_2Cl_2:TFE::1:4) and mixed with 300 μl of BSA or dye (in distilled water), forming a clear, single phase solution, which was added to 200 mL of non-solvent (5% PVA). The emulsion formed spontaneously and was allowed to stir at room temperature for 3 h. The microspheres were collected by centrifugation, washed 3 times with distilled water and lyophilized. Microspheres were stored at −20 °C with desiccant until use. For the larger sized microspheres, all conditions were held except the co-solvent ratio was changed to CH_2Cl_2:TFE::3:2.

2.3. Microsphere size distribution

Size distribution of microspheres was determined using Coulter LS 230 software (Version 3.01) on a LS 230 Coulter Counter (Beckman Coulter, Hialeah, FL).

2.4. Scaffold fusion

Microspheres were fused into 3D scaffolds using a teflon mold. Four to twenty milligrams of microspheres were added to the disc-like mold (6 mm in diameter) and placed inside a sealed glass chamber (137.6 mL volume) containing 3 mL of dichloromethane. The chamber was sealed and microspheres were allowed to fuse for various time intervals. After fusion the mold containing the scaffold was removed from the chamber and allowed to air for 10 min at room temperature, at which point the scaffold was removed from the mold and dried under vacuum overnight. All scaffolds were stored at −20 °C with desiccant until use.

2.5. Morphology

Microsphere and scaffold morphology was imaged by the Hitachi 2700 scanning electron microscope (SEM, Tokyo, Japan) at 5 kV. All samples were secured to the stub using carbon tape, and were sputter coated with PdAu for 4 min at 20 mA using the EMITECH K550 Sputter Coater (Houston, TX).

Digital images of scaffolds and mold were obtained with Mamiya 645 AFD II camera (Elmsford, NY) with a 120 mm f/4 macro lens, a macro bellows, and a digital capture back.

2.6. Release study

Microsphere and scaffold release studies were carried out in phosphate buffered saline (PBS, pH 7.2) at 37 °C. Ten milligrams of microspheres were incubated with 1 mL PBS in capped tubes and placed on a rotator. For scaffolds, 10 mg-sized scaffolds were placed in a 24 well plate with 1 mL of PBS per scaffold and placed on an orbital shaker. At each time

point (1, 2, 4, 10, 14, 21 and 28 days), the releasate was removed and stored at −80 °C until analysis. A fresh 1 mL of PBS was added to samples and they were re-incubated until the following time point. Amount of BSA released from the samples was quantified using the micro BCA assay (Pierce, Rockford, IL). All samples were run in triplicate and data points are shown as mean ± standard deviation. To determine significance ($p < 0.05$), two-tailed t-test was performed assuming unequal variances.

2.7. Cell attachment study

Scaffolds were pre-wetted with media (Eagle's Basal Medium with 2 mM L-glutamine, 10% FBS) and incubated at 37 °C 5% CO_2. After 12 h, the media was aspirated and 10T1/2 cells (ATCC, Manassas, VA) were added directly to each scaffold in 20 μL media suspension (1×10^6 cells/28.3 mm^3 scaffold volume). After 2 h, 2 mL of media was slowly added to each well without disturbing the scaffold. The plate was incubated on an orbital shaker for an additional 2 h.

Seeded scaffolds were prepared for SEM analysis by first rinsing three times in PBS. Then, the samples were placed in 2.5% glutaraldehyde (Electron Microscopy Sciences, Hatfield, PA) in cacodylate buffer for 1 h, after which, the samples were rinsed in distilled water and then dehydrated in a series of ethanol washes (50%, 75%, 95%, and 100%). Finally, the seeded scaffolds were soaked twice in hexamethyldisilazine (HMDS, Sigma, St. Louis, MO) for 5 min. The fixed scaffolds were then placed on a SEM stub and coated for imaging as described in Section 2.5.

3. Results and discussion

3.1. Scaffold fusion

Microspheres fabricated for the scaffold fusion experiments were mostly less than 20 μm and the mean size was not significantly different between the formulations (Table 1). Thus, for the percentages tested, BSA loading has no significant effect on microsphere size. Furthermore, Fig. 1a shows that 4.3% BSA loaded microspheres are well formed and with no evidence of aggregation.

The scaffolds fabricated were all disks about 6 mm in diameter and 1–2 mm in height. While this was the desired mold for our studies, simply changing the mold can easily alter the shape of the scaffold. This scaffold fabrication process relies on dichloromethane diffusion into the microspheres, which lowers the polymer glass transition temperature (T_g), thus allowing microsphere fusion. In this particular study, we wanted to determine the optimal scaffold fusion time by controlling the microsphere exposure time to dichloromethane vapors. Fig. 1 shows the morphology of scaffolds for various fusion times. For these samples the microsphere composition (4.3% BSA) and mass were held constant. It is clear that in this experiment, after 4 min (Fig. 1c) the microspheres start to fuse together, after 4 min and 30 s (Fig. 1e) the scaffold is over fused, finally turning into a film after 5 min (Fig. 1f). The desirable scaffold structure or ideal fusion is representative of the sample in Fig. 1d. The spheres are fused together but their underlying structure is still visible, and the entire scaffold is easy to handle and transport with a spatula or forceps. This fusion method utilizes the dichloromethane vapor diffusion to lower the polymer glass transition temperature and soften the polymer microspheres after which they fuse together. After the dichloromethane is eliminated, the polymer hardens again while preserving the fused structure. Once the fusion chamber has reached saturation vapor pressure for dichloromethane, the reaction is rather fast, as seen in Fig. 1e and f, where the microspheres fuse into a film in about 1 min. At this point in the process, the dichloromethane has sufficiently penetrated throughout the entire microsphere matrix reducing the polymer T_g, whereas at earlier time stages only the microsphere surface was affected.

Several observations were made regarding the scaffold fusion time, including the effect of microsphere mass on fusion time. Ideal fusion time was identified qualitatively as the point at which the scaffold had a connected network of microspheres but still retained its porous shape (i.e. the point just prior to densification). Fig. 2 summarizes the results of fusing 2, 10 and 20 mg scaffolds for 4, 9 and 10:30 min, respectively. It is clear that fusion time increases for scaffold mass. This is expected because the fusion process is governed by dicholoromethane vapor diffusion and added mass generally indicates longer diffusion time. Since mass is an important factor in this process, for each subsequent experiment the microsphere mass was held constant between groups.

Keeping the fusion time and amount of microspheres constant, the effect of protein loading on the extent of fusion was studied (Fig. 3). Ten milligrams of microspheres loaded with 4.3% BSA (Fig. 3a and d), 1.5% BSA (Fig. 3b and e) and 0.4% BSA (Fig. 3c and f) were all fused for 9 min. As evidenced by SEM analysis, under these conditions the microspheres containing the least amount of BSA fused the most while those with the highest amount of BSA fused the least, showing that when fusion time and mass are held constant, the fusion process is more pronounced for samples with less BSA. This phenomenon is not a function of the amorphous PLGA and the low T_g, but of the BSA, which may be more ordered and acts as reinforcement for the soft microspheres, thus requiring

Table 1
Size distribution of BSA loaded microspheres

BSA loading (%)	Mean (μm)	90% < (μm)
0	7.7 ± 7.4	17.3
0.4	6.4 ± 6.5	14.3
1.5	7.3 ± 8.3	16.1
4.3	9.4 ± 12.1	19.6

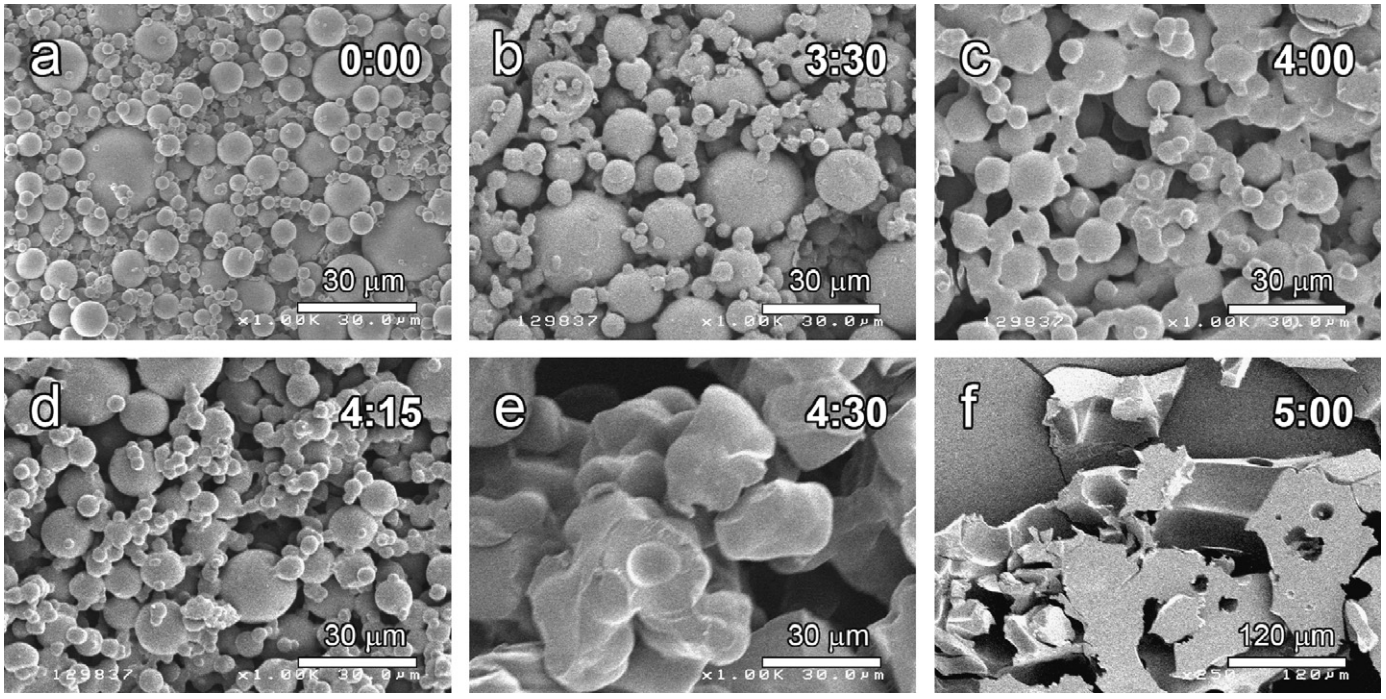

Fig. 1. Scanning electron microscope images of microspheres fused for 0 (a), 3:30 (b), 4:00 (c), 4:15 (d), 4:30 (e) and 5:00 (f) minutes. Microsphere composition (4.3% BSA), mass (2 mg) and fusion conditions were held constant. Scale bar is 30 μm, except (f) is 120 μm.

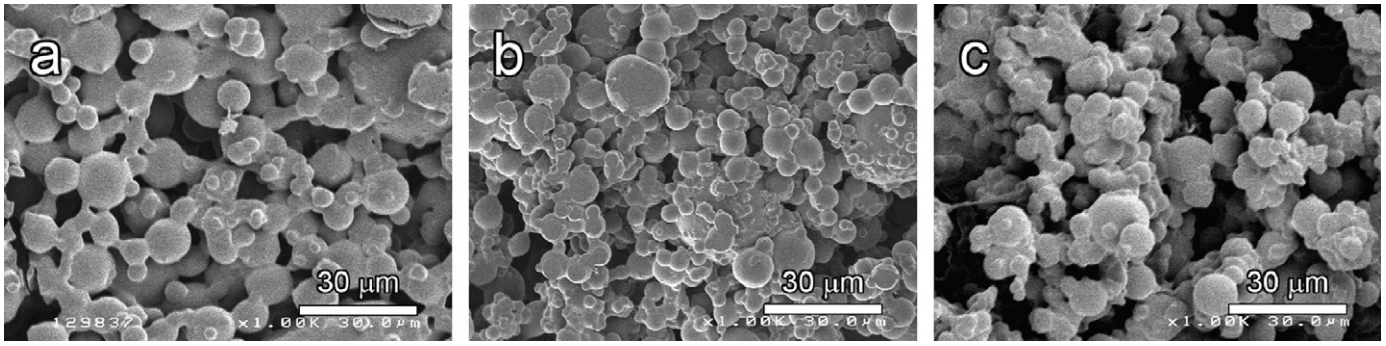

Fig. 2. Scanning electron micrographs of optimal scaffolds where microsphere mass and fusion time was varied. Fusion time (min) and mass (mg) are (a) 4:00/2, (b) 9:00/10, (c) 10:30/20, respectively. All scaffolds were made from 4.3% BSA-loaded microspheres. Scale bar is 30 μm.

more vapor for fusion. In this case, the polymer glass transition temperature does not differ across the 0.4%, 1.5% and 4.3% BSA loaded microspheres, however the vapor needed to cause fusion over the entire structure (polymer plus BSA) does increase. Also, the secondary interactions between the PLGA (-COOH terminated) and BSA chins could contribute to microsphere stability, thus requiring more vapor to soften the microsphres and allow for chain movement between the spheres [36].

Overall, the fusion time was found to be a controlling factor in the fabrication of these scaffolds. The extent of fusion displayed by the scaffolds increased as the amount of fusion time increased. The amount of fusion time required for optimum scaffold morphology also increased with increased protein loading and increased microsphere mass.

3.2. Protein release from scaffolds

To evaluate the effect of the fusion process on protein release rates, we compared BSA released from scaffolds with unfused microspheres (Fig. 4). Release from two types of scaffolds was studied, one fused for 10 min and one for 10:30 min. Over the 20-day study, the BSA released was not significantly different between the scaffolds ($p > 0.05$ for all time points), indicating that increasing fusion time by 30 s does not affect scaffold release even though it could significantly alter scaffold morphology (Fig. 1). Comparing BSA release between loose microspheres and scaffold fused for 10:30 min, we see that for the first week of release (time points day 1, 2, 4 and 7) there is significantly higher release ($p < 0.05$) for the loose microspheres. In addition, when comparing loose

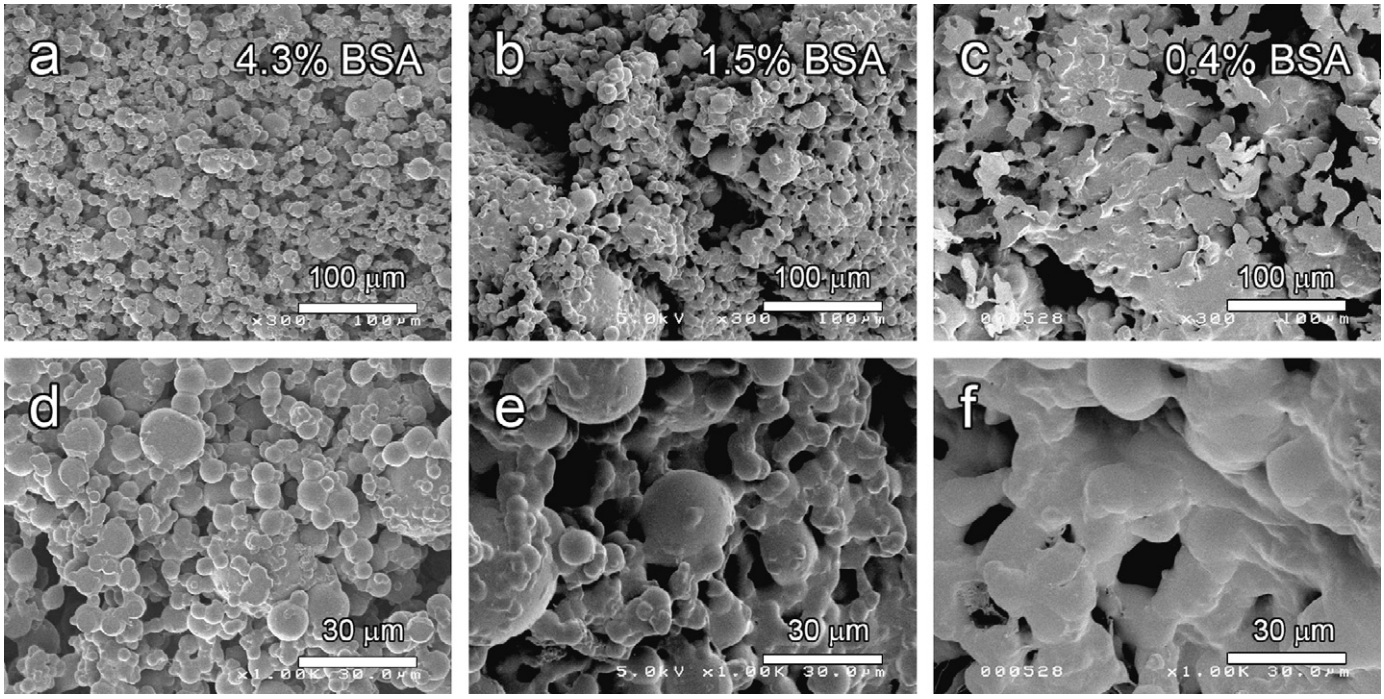

Fig. 3. Scanning electron microscope images of scaffolds made from microspheres loaded with 4.3% BSA (a and d), 1.5% BSA (b and e) and 0.4% BSA (c and f). All other fusion parameters were held constant. Scale bar is 100 μm for the top row and 30 μm for the bottom row.

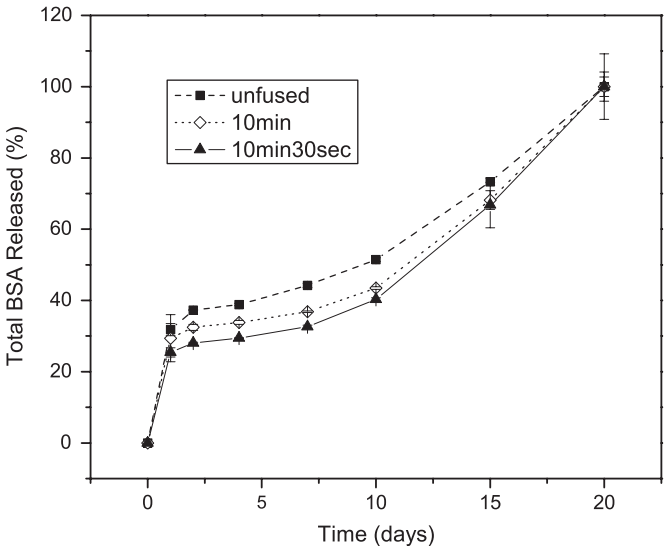

Fig. 4. Percent cumulative release of BSA from unfused 4.3% loaded microspheres (■), scaffolds fused for 10 min (◇), and scaffolds fused for 10:30 min (▲). Scaffolds were made from 4.3% BSA loaded microspheres and all other fusion parameters were held constant.

microspheres to scaffold fused for 10 min, the microspheres release significantly more ($p<0.05$) on day 7 only. However, the unfused microspheres cumulatively released the same amount (100 μg) of BSA as the scaffolds, and the slopes of the release curves after day 10 were not significantly different, indicating identical rates of release. The difference in BSA release between loose microspheres and scaffolds can be attributed to the reduction in surface area after fusion. While not physically measured, SEM analysis indicates that scaffold formation occurs when two or more microspheres fuse with each other by overlapping. Since the overall scaffold volume does not increase over fusion time, it can be shown mathematically [37] that scaffold surface area is lower than that of the loose microspheres for a given mass. These results show that the release rates obtained from microsphere formulations can predict the corresponding scaffold release rates. This can aid in designing scaffolds with sequential growth factor release by fine tuning the microsphere release kinetics prior to scaffold fabrication. Moreover, we show elsewhere that growth factors can be encapsulated and released from our microspheres in bioactive form, and can subsequently be fused into scaffolds that release them at corresponding rates as determined by growth factor specific ELISAs [38]. Additionally, with respect to microspheres, the unloaded control degraded 6 times more quickly than the 4.3% protein loaded microspheres (data not shown), suggesting that incorporating BSA in the microspheres, and thereby in the scaffolds, stabilizes the constructs longer under these conditions.

3.3. Scaffold composition

In order to demonstrate the versatility of this scaffold fabrication method, 4.3% of various dyes were encapsulated in PLGA microspheres for visual effect. Fig. 5a shows an image of a 20 mg scaffold composed equally of acid green, red 27, and fast green FCF microspheres.

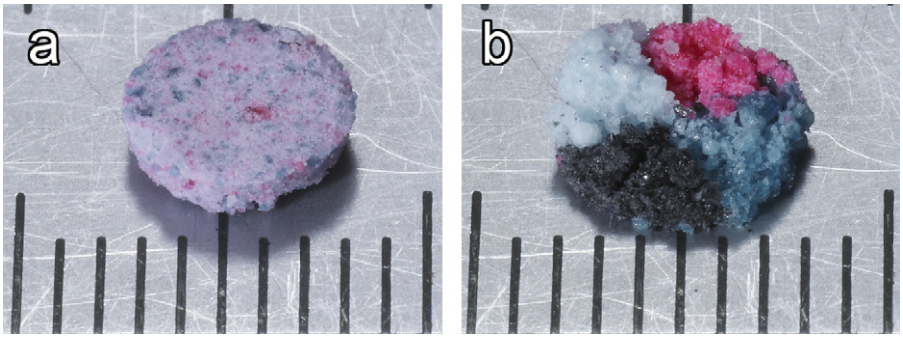

Fig. 5. Microspheres loaded with dyes fused into scaffolds after mixing acid green, red 27, and fast green FCF containing microspheres together (a) and after positioning carbon black, acid green, red 27, and fast green FCF microspheres clockwise into 4 sections (b).

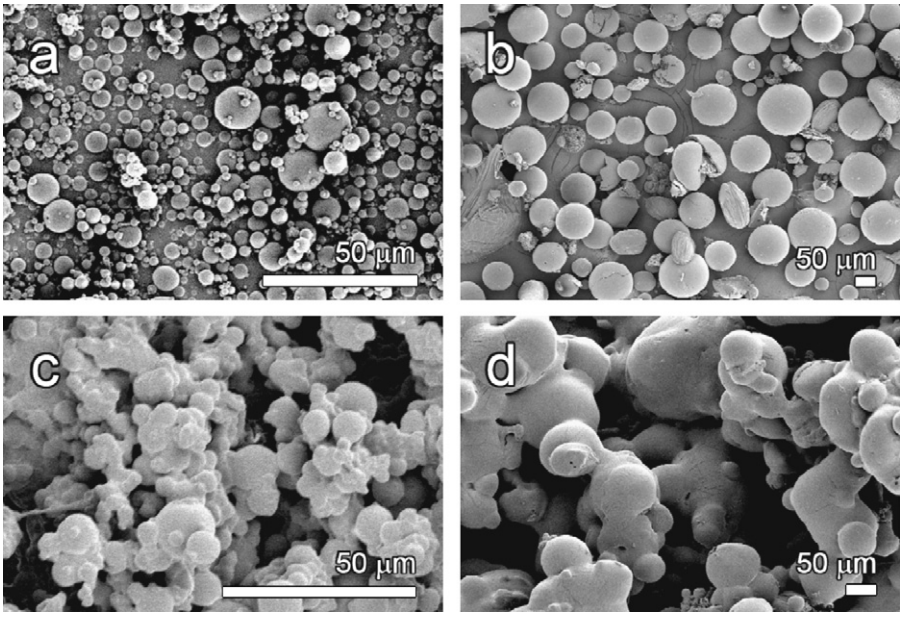

Fig. 6. Scanning electron microscope images of (a) small ($11.15 \pm 11.08\,\mu m$) and (b) large ($113.3 \pm 58.0\,\mu m$) microspheres and the resulting scaffolds after fusion (c) and (d), respectively. Scale bars are 50 μm.

The colored microspheres were mixed with a spatula and fused into a scaffold containing a well-dispersed lavender colored distribution. Some minor color aggregation does occur throughout the scaffold, but this can be remedied with mechanical mixing and reduced static. In Fig. 5b, 4.3% dye loaded microspheres were fused in a pie chart like arrangement. This produced a scaffold with spatially distinct regions of carbon black (Fig. 5b, clockwise), acid green, red 27, and fast green FCF. These results indicate just how malleable these scaffolds are, as they can contain anything that can be encapsulated within microspheres. Thus, the spatial distribution and composition of microspheres can be controlled within the 3D scaffold, which has been shown to be important for controlled angiogenesis [39]. Furthermore, various polymers can be fused such as capped PLGA, uncapped PLGA and PLLA (data not shown), allowing for additional control over scaffold degradation.

3.4. Cell attachment to scaffolds

A requirement of scaffold design for tissue engineering applications is allowing enough void volume for cell seeding and proliferation prior to scaffold degradation, in addition to using biocompatible materials. The data presented above was obtained with relatively small sized microspheres (see Table 1), which after fusion resulted in scaffolds of about 20 μm pores. In order to increase the size of the microspheres we changed the co-solvent ratio (CH_2Cl_2:TFE) of the organic phase in the SE method from 1:4 to 3:2, yielding relatively small ($11.15 \pm 11.08\,\mu m$) and large ($113.3 \pm 58.0\,\mu m$) microspheres, respectively (Fig. 6a and b). These microspheres were subsequently fused into scaffolds, as shown in Fig. 6c and d for 8 and 10:30 min, respectively. The different fusion times were necessary in order to obtain optimally fused scaffolds since smaller microspheres fuse into scaffolds faster than larger

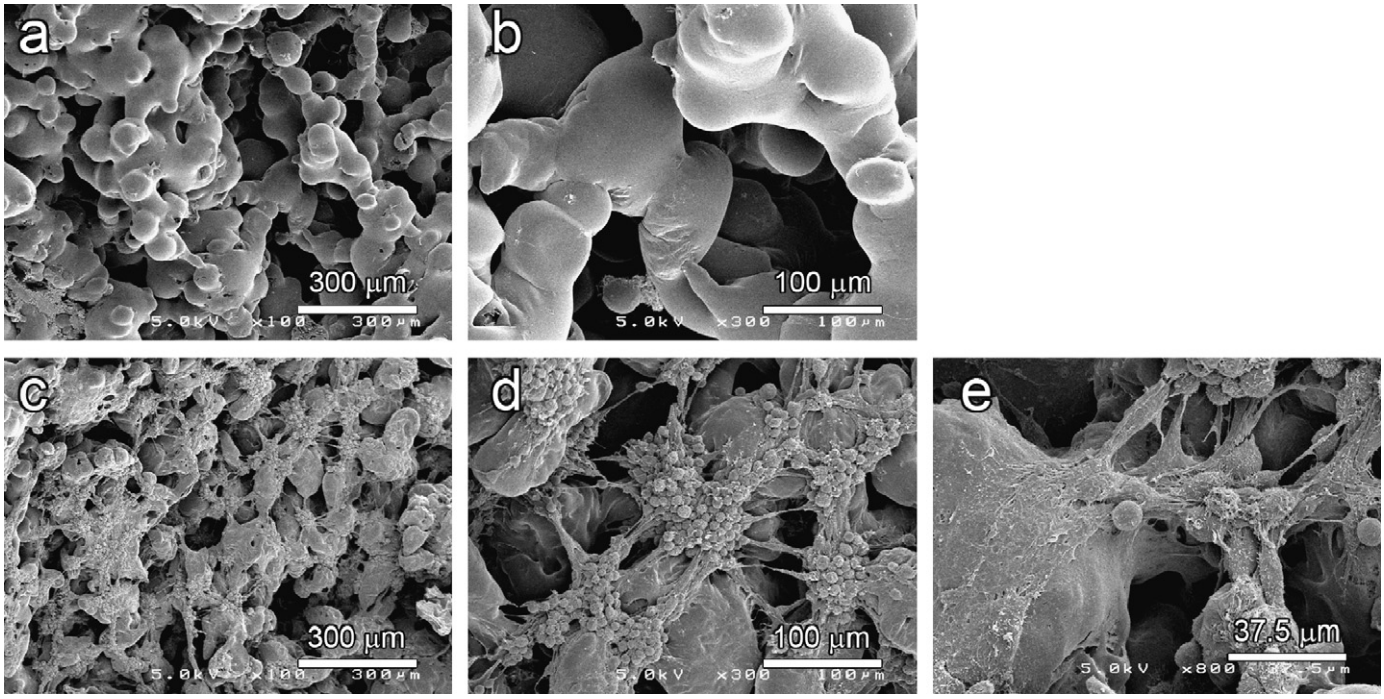

Fig. 7. Scanning electron microscope images of scaffolds alone (a and b) and seeded with fibroblast cells (c, d and e). Scale bars are (a and c) 300 μm, (b and d) 100 μm and (e) 37.5 μm.

ones. This is attributed to the fact that for constant mass there is less surface area available for larger microspheres as compared to smaller ones per scaffold. Therefore, more time is needed with larger microspheres for dichloromethane vapor to diffuse into the microspheres and soften the polymer enough allowing chain movement to occur. The pores within the scaffolds made of small and large spheres are on the order of 20 and 200 μm, respectively. This indicates that by increasing the mean microsphere size tenfold, the resultant scaffold pore sizes can be increased by the same factor. The mechanism here is most likely similar to that of sintering [40,41], where particles of large size distributions lead to more porous structure because the large microspheres tend to engulf smaller ones, thus generating larger pores between particles. This phenomenon introduces even more flexibility into the scaffold fabrication method by allowing for control over scaffold pore size.

In order to test the ability of these scaffolds to act as cell carriers, a cell attachment study was performed on scaffolds made from large microspheres (113.3 ± 58.0 μm). Fibroblast cells were seeded onto pre-wetted scaffolds and, after 4 h of incubation, cell attachment was evaluated by SEM. Fig. 7 shows SEM images of both empty and seeded scaffolds. The cells are attached across the entire scaffold surface and some have formed bridges across the pores (Fig. 7c and d). In addition, cells also penetrated and attached well inside the pores (Fig. 7e). Flat cell morphology is prevalent among cells attached directly to the polymer surface (Fig. 7e), while the balled-like appearance is present in cells residing on top of other fibroblasts. These images show that the scaffolds are favorable to cell attachment and are compatible with the fibroblast cells used for this experiment.

4. Conclusion

We have developed a novel and simple vapor fusion method for generating 3D scaffolds from protein-loaded microspheres. We have successfully shown that by varying process parameters we can control scaffold morphology, composition, spatial distribution, pore size, and protein release kinetics. The versatility of these scaffolds to carry cells and contain essentially any number/combination of loaded microsphere makes them strong candidates for use in tissue engineering applications and therapeutic localized drug delivery.

Acknowledgments

The authors would like to thank Dr. Moses Goddard for taking the digital photographs and Dr. Bahar Bilgen for editing the manuscript. This work was supported in part by the Vice President of Research Seed Grant, Brown University.

References

[1] Langer R, Vacanti JP. Tissue engineering. Science 1993;260(5110):920–6.
[2] Lee KY, Peters MC, Anderson KW, Mooney DJ. Controlled growth factor release from synthetic extracellular matrices. Nature 2000;408(6815):998–1000.

[3] Levenberg S, Huang NF, Lavik E, Rogers AB, Itskovitz-Eldor J, Langer R. Differentiation of human embryonic stem cells on three-dimensional polymer scaffolds. Proc Natl Acad Sci USA 2003; 100(22):12741–6.
[4] Teng YD, Lavik EB, Qu X, Park KI, Ourednik J, Zurakowski D, et al. Functional recovery following traumatic spinal cord injury mediated by a unique polymer scaffold seeded with neural stem cells. Proc Natl Acad Sci USA 2002;99(5):3024–9.
[5] Frenkel SR, Di Cesare PE. Scaffolds for articular cartilage repair. Ann Biomed Eng 2004;32(1):26–34.
[6] Hunziker EB. Articular cartilage repair: basic science and clinical progress. A review of the current status and prospects. Osteoarthritis Cartilage 2002;10(6):432–63.
[7] Tabata Y. Tissue regeneration based on growth factor release. Tissue Eng 2003;9(Suppl 1):S5–S15.
[8] Caplan AI, Elyaderani M, Mochizuki Y, Wakitani S, Goldberg VM. Principles of cartilage repair and regeneration. Clin Orthop Relat Res 1997(342):254–69.
[9] Camarata PJ, Suryanarayanan R, Turner DA, Parker RG, Ebner TJ. Sustained release of nerve growth factor from biodegradable polymer microspheres. Neurosurgery 1992;30(3):313–9.
[10] DeFail AJ, Chu CR, Izzo N, Marra KG. Controlled release of bioactive TGF-beta 1 from microspheres embedded within biodegradable hydrogels. Biomaterials 2006;27(8):1579–85.
[11] Edelman ER, Mathiowitz E, Langer R, Klagsbrun M. Controlled and modulated release of basic fibroblast growth factor. Biomaterials 1991;12(7):619–26.
[12] Hosseinkhani H, Hosseinkhani M, Khademhosseini A, Kobayashi H, Tabata Y. Enhanced angiogenesis through controlled release of basic fibroblast growth factor from peptide amphiphile for tissue regeneration. Biomaterials 2006;27(34):5836–44.
[13] Kawai K, Suzuki S, Tabata Y, Ikada Y, Nishimura Y. Accelerated tissue regeneration through incorporation of basic fibroblast growth factor-impregnated gelatin microspheres into artificial dermis. Biomaterials 2000;21(5):489–99.
[14] Miyamoto S, Takaoka K, Okada T, Yoshikawa H, Hashimoto J, Suzuki S, et al. Polylactic acid-polyethylene glycol block copolymer. A new biodegradable synthetic carrier for bone morphogenetic protein. Clin Orthop Relat Res 1993(294):333–43.
[15] Richardson TP, Peters MC, Ennett AB, Mooney DJ. Polymeric system for dual growth factor delivery. Nat Biotechnol 2001;19(11):1029–34.
[16] Yuksel E, Weinfeld AB, Cleek R, Jensen J, Wamsley S, Waugh JM, et al. Augmentation of adipofascial flaps using the long-term local delivery of insulin and insulin-like growth factor-1. Plast Reconstr Surg 2000;106(2):373–82.
[17] Yuksel E, Weinfeld AB, Cleek R, Wamsley S, Jensen J, Boutros S, et al. Increased free fat-graft survival with the long-term, local delivery of insulin, insulin-like growth factor-I, and basic fibroblast growth factor by PLGA/PEG microspheres. Plast Reconstr Surg 2000;105(5):1712–20.
[18] Kim K, Fisher JP. Nanoparticle technology in bone tissue engineering. J Drug Target 2007;15(4):241–52.
[19] Na K, Kim SW, Sun BK, Woo DG, Yang HN, Chung HM, et al. Osteogenic differentiation of rabbit mesenchymal stem cells in thermo-reversible hydrogel constructs containing hydroxyapatite and bone morphogenic protein-2 (BMP-2). Biomaterials 2007;28(16): 2631–7.
[20] Ma PX, Elisseeff JH. Scaffolding in tissue engineering. Boca Raton: Taylor & Francis; 2005.
[21] Aebischer P, Salessiotis AN, Winn SR. Basic fibroblast growth factor released from synthetic guidance channels facilitates peripheral nerve regeneration across long nerve gaps. J Neurosci Res 1989;23(3):282–9.
[22] Arm DM, Tencer AF, Bain SD, Celino D. Effect of controlled release of platelet-derived growth factor from a porous hydroxyapatite implant on bone in growth. Biomaterials 1996;17(7):703–9.
[23] DeBlois C, Cote MF, Doillon CJ. Heparin-fibroblast growth factor-fibrin complex: *in vitro* and *in vivo* applications to collagen-based materials. Biomaterials 1994;15(9):665–72.
[24] Heckman JD, Boyan BD, Aufdemorte TB, Abbott JT. The use of bone morphogenetic protein in the treatment of non-union in a canine model. J Bone Joint Surg Am 1991;73(5):750–64.
[25] Hong L, Tabata Y, Yamamoto M, Miyamoto S, Yamada K, Hashimoto N, et al. Comparison of bone regeneration in a rabbit skull defect by recombinant human BMP-2 incorporated in biodegradable hydrogel and in solution. J Biomater Sci Polym Ed 1998;9(9):1001–14.
[26] Lee M, Chen TT, Iruela-Arispe ML, Wu BM, Dunn JC. Modulation of protein delivery from modular polymer scaffolds. Biomaterials 2007;28(10):1862–70.
[27] Nillesen ST, Geutjes PJ, Wismans R, Schalkwijk J, Daamen WF, van Kuppevelt TH. Increased angiogenesis and blood vessel maturation in acellular collagen-heparin scaffolds containing both FGF2 and VEGF. Biomaterials 2007;28(6):1123–31.
[28] Ozeki M, Ishii T, Hirano Y, Tabata Y. Controlled release of hepatocyte growth factor from gelatin hydrogels based on hydrogel degradation. J Drug Target 2001;9(6):461–71.
[29] Park YJ, Lee YM, Park SN, Sheen SY, Chung CP, Lee SJ. Platelet derived growth factor releasing chitosan sponge for periodontal bone regeneration. Biomaterials 2000;21(2):153–9.
[30] Ripamonti U, Bosch C, van den Heever B, Duneas N, Melsen B, Ebner R. Limited chondro-osteogenesis by recombinant human transforming growth factor-beta 1 in calvarial defects of adult baboons (Papio ursinus). J Bone Miner Res 1996;11(7):938–45.
[31] Stewart K, Pabbruwe M, Dickinson S, Sims T, Hollander AP, Chaudhuri JB. The effect of growth factor treatment on meniscal chondrocyte proliferation and differentiation on polyglycolic acid scaffolds. Tissue Eng 2007;13(2):271–80.
[32] Tabata Y, Miyao M, Ozeki M, Ikada Y. Controlled release of vascular endothelial growth factor by use of collagen hydrogels. J Biomater Sci Polym Ed 2000;11(9):915–30.
[33] Takaoka K, Koezuka M, Nakahara H. Telopeptide-depleted bovine skin collagen as a carrier for bone morphogenetic protein. J Orthop Res 1991;9(6):902–7.
[34] Reed AM, Gilding DK. Biodegradable polymers for use in surgery-poly(lactic)/poly(glycolic acid) homo and copolymers: 2. *In vitro* degradation. Polymer 1981;22:494–8.
[35] Fu K, Harrell R, Zinski K, Um C, Jaklenec A, Frazier J, et al. A potential approach for decreasing the burst effect of protein from PLGA microspheres. J Pharm Sci 2003;92(8):1582–91.
[36] Ageorges C, Ye L, Hou M. Advances in fusion bonding techniques for joining thermoplastic matrix composites: a review. Composites: Part A: Appl Sci Manuf 2001;32:839–57.
[37] Eggers J. Coalescence of spheres by surface diffusion. Phys Rev Lett 1998;80(12):2634–7.
[38] Jaklenec A, Hinckfuss A, Ciombor DM, Aaron R, Mathiowitz E. Sequential release from PLGA scaffolds fused from bioactive IGF-I and TGF-β1 microspheres. Biomaterials 2007; under review.
[39] Chen RR, Silva EA, Yuen WW, Mooney DJ. Spatio-temporal VEGF and PDGF delivery patterns blood vessel formation and maturation. Pharmaceut Res 2007;24(2):258–64.
[40] Wang YU. Computer modeling and simulation of solid-state sintering: a phase field approach. Acta Mater 2006;54:953–61.
[41] Kingery WD, Bowen HK, Uhlmann DR. Introduction to ceramics. 2nd ed. New York: Wiley; 1976.